

Supporting Information

Highly Conductive, Transparent Molecular Charge-Transfer Salt with Reversible Lithiation

Ying-Shi Guan^{1,2}, Yong Hu^{1,2}, Hanguang Zhang³, Gang Wu^{3*}, Hao Yan^{4*}, Shenqiang Ren^{1,2*}

1 Department of Mechanical and Aerospace Engineering, University at buffalo, The State University of New York, Buffalo, NY, 14260, USA

2 Research and Education in eNergy, Environment and Water (RENEW) Institute, University at buffalo, The State University of New York, Buffalo, NY, 14260, USA

3 Department of Chemical and Biological Engineering, University at Buffalo, The State University of New York, Buffalo, NY 14260, USA

4 Center for High Pressure Science and Technology Advanced Research, Shanghai, 201203, P.R. China

*e-mail: shenren@buffalo.edu

gangwu@buffalo.edu

yanhao@hpstar.ac.cn

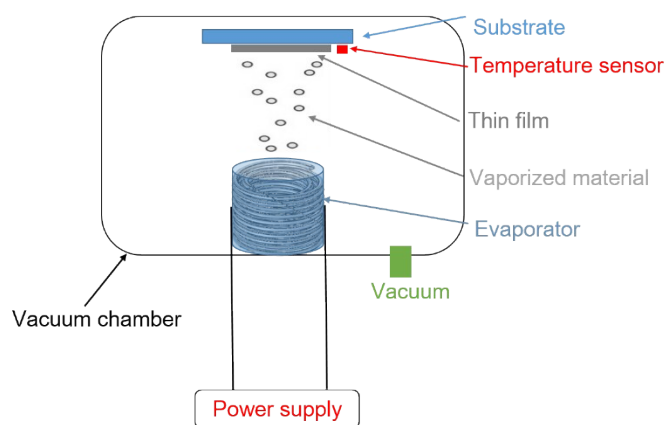
Experimental Section

Materials and instruments. TTF and TCNQ purchased from Sigma-Aldrich and used as received. The SEM images were taken from FEI Quanta450FEG. UV-Vis spectra were recorded on an Agilent Model HP8453 UV-vis spectrophotometer. I–V characteristics of the bulk samples and thin films were recorded with a Keithley 2400 semiconductor analyzer. A Bruker Apex II Duo single-crystal X-ray diffractometer was used to obtain the XRD pattern at a step of 0.1° per minute from 3° to 30° . The in-situ synchrotron X-ray diffraction measurements were performed at the PLS-II 9A U-SAXS beamline of the Pohang Accelerator Laboratory (Korea). The operating conditions were set at the x-ray energy of 19.79 KeV. The XRD patterns were recorded using a 2D CCD detector (SX-165, Rayonix) with an exposure time of 60 seconds.

The fabrication of the TTF-TCNQ bulk pellets. TTF-TCNQ complex was synthesized by mixing equimolar hot acetonitrile solutions of TTF and TCNQ. Adding the TCNQ solution into TTF solution drop by drop, the shiny black crystals were precipitated immediately. After cooling slowly overnight, the black crystals were collected by filtration, then washed several times using acetonitrile to purify the TTF-TCNQ complex. The obtained black crystals were dried in vacuum. The TTF-TCNQ complex were ground and pressed by a mold with diameter of 10 mm in 9 ton.

The fabrication of the TTF-TCNQ thin films. The TTF-TCNQ thin films were fabricated by evaporate the purified TTF-TCNQ complex mentioned above using an in-house apparatus. A metal wire conneted with power supply was used as heater to heat the evaporator. The chamber vacuumed by a pump. A commercial temperature

sensor can be used to monitor the substrate temperature. The detailed structure depicted in the following schematic diagram. The TTF-TCNQ thin films with different thickness were deposited on glass slides through controlling the evaporation time.



Schematic diagram for the vacuum deposition apparatus.

Electrical characterization of the TTF-TCNQ thin Films. The temperature dependent resistance of the TTF-TCNQ thin films were measured by the standard four-point probe method using an in-house apparatus. The temperature can be controlled from 50 K to 400 K.

The fabrication of photodetector. The PEDOT:PSS was spun coated on glass substrates at 3000 rpm for 60 s. The obtained film was immersed in concentrated H_2SO_4 solutions for 12h at room temperature. Then the films were washed with deionized water several times and dried at 120 °C for 30mins to remove residual water completely. Subsequently, the P3BT- C_{60} film was transferred onto the PEDOT:PSS. At last, TTF-TCNQ thin film was evaporated as electrode.

Electrochemical characterization. Electrochemical properties of the materials were evaluated in 2032 coin cells using Li metal as the counter electrode. For electrode fabrication, Vapor deposition was used to prepare electrodes without any addition of

binder and carbon conductor. TCNQ-TTF was vaporized and deposited on the Cu substrate. Coin cell assembly was conducted inside an argon-filled glove box (O_2 and $H_2O < 0.1$ ppm). A mixture of 1 M Lithium hexafluorophosphate in dimethyl carbonate and ethylene carbonate in a ratio of 1:1 (by volume) was used as the electrolyte. The galvanostatic cycling test were recorded within a potential window of 0.05 to 3.0 V (vs Li/Li^+) at the current density of 20 mA/g using an Arbin battery tester.

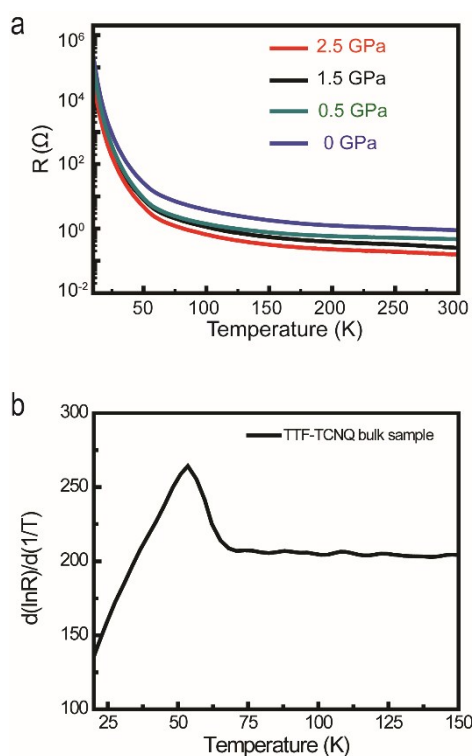


Figure S1. (a) The temperature-dependent resistance of the TTF–TCNQ bulk samples under different pressures. (b) The dependence of resistivity derivative for TTF-TCNQ bulk samples used to define the Peierls transition.

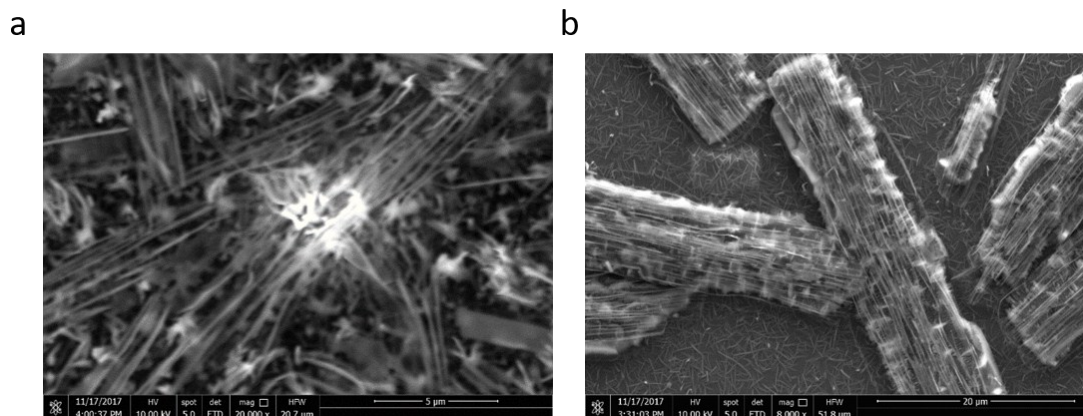


Figure S2. The SEM images of the TTF-TCNQ film with different thickness (500 nm for a and 1000 nm for b).

Electron Image 1

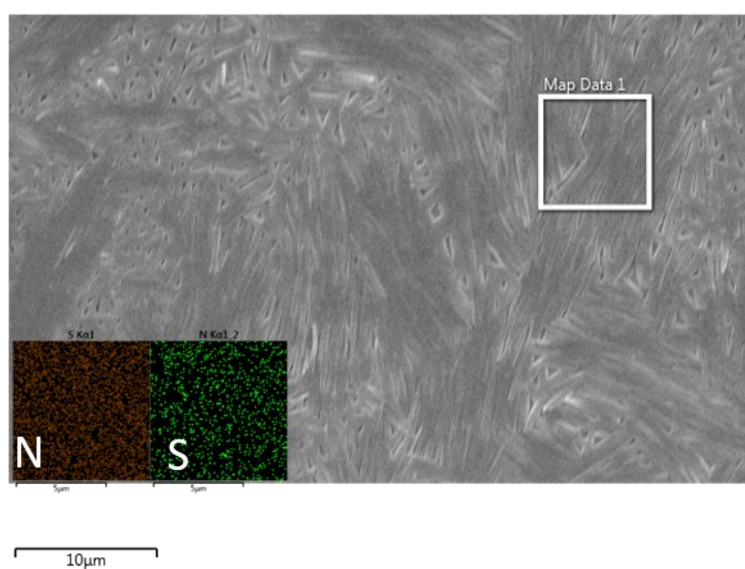


Figure S3. The SEM images and EDS mapping of the TTF-TCNQ film with thickness of 190 nm.

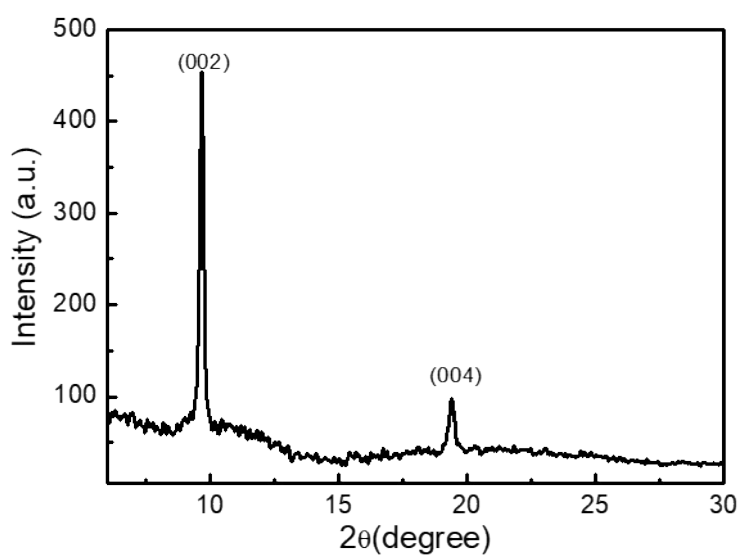


Figure S4. The XRD of the TTF-TCNQ film.

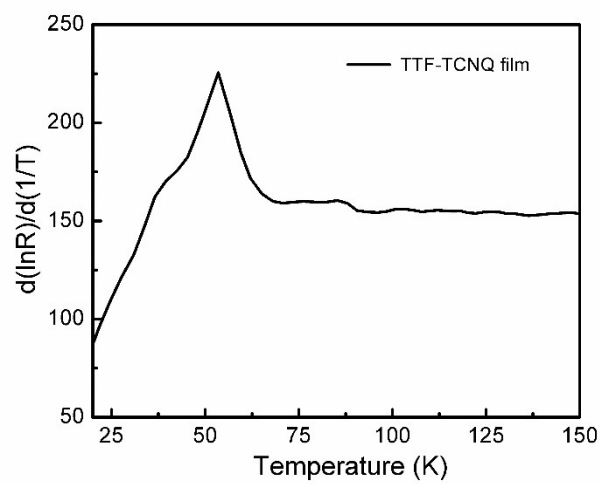


Figure S5. The dependence of resistivity derivative for TTF-TCNQ film sample used to define the Peierls transition.

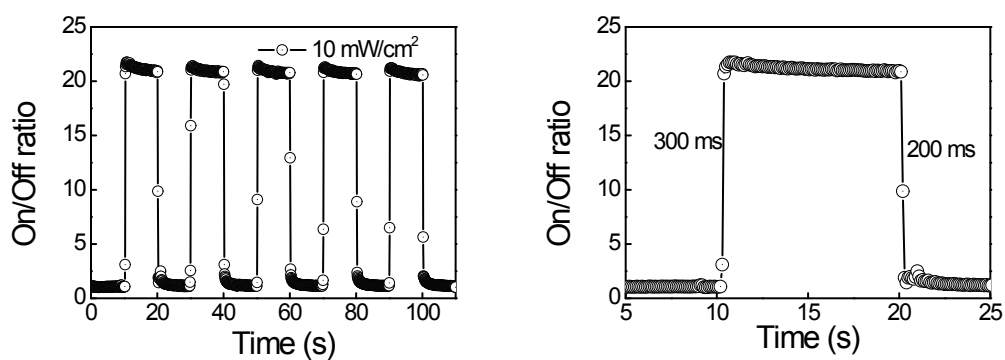


Figure S6. The current on/off ratio was normalized by the dark current (left), and the response time of the photodetectors measured under illumination of 10 mW/cm² using TTF-TCNQ film as the electrode.

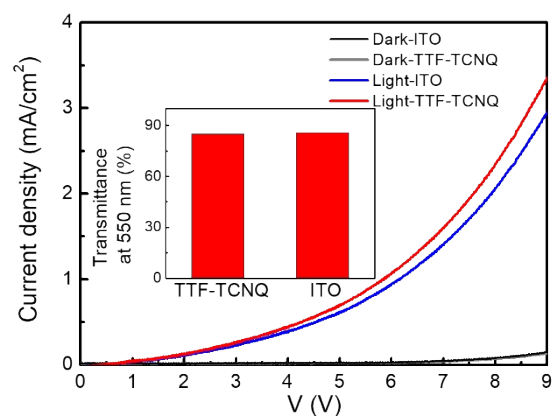
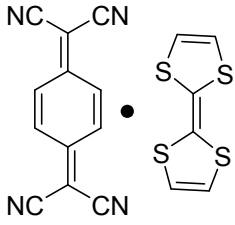
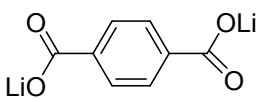
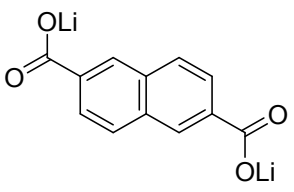
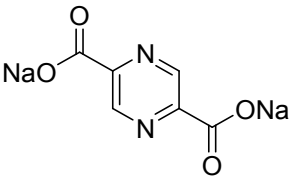
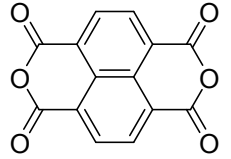
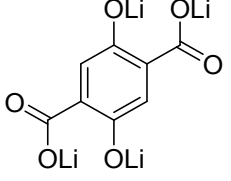
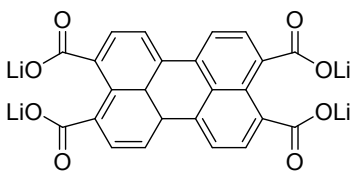


Figure S7. The current-voltage (I-V) characteristics of photodetectors measured under illumination of 10 mW/cm² using TTF-TCNQ film and ITO as the electrode respectively.

Table S1. Summary the performance of small organic molecules as anodes for lithium-ion batteries.

Anode materials	Current density	Specific capacity, cycles	Reference
	20 mA/g	250 mAh/g, 90	This work
	15 mA/g	234 mAh/g, 50	3
	12 mA/g	115 mAh/g, 50	4
	20 mA/g	210 mAh/g, 200	5
	100 mA/g	900 mAh/g, 30	6
	24 mA/g	232 mAh/g, 50	7
	50 mA/g	170 mAh/g, 50	8

References:

- [1] A. C. Ferrari, F. Bonaccorso, V. Fal'ko, K. S. Novoselov, S. Roche, P. Boggild, S. Borini, F. H. L. Koppens, V. Palermo, N. Pugno, J. A. Garrido, R. Sordan, A. Bianco, L. Ballerini, M. Prato, E. Lidorikis, J. Kivioja, C. Marinelli, T. Ryhanen, A. Morpurgo, J. N. Coleman, V. Nicolosi, L. Colombo, A. Fert, M. Garcia-Hernandez, A. Bachtold, G. F. Schneider, F. Guinea, C. Dekker, M. Barbone, Z. Sun, C. Galiotis, A. N. Grigorenko, G. Konstantatos, A. Kis, M. Katsnelson, L. Vandersypen, A. Loiseau, V. Morandi, D. Neumaier, E. Treossi, V. Pellegrini, M. Polini, A. Tredicucci, G. M. Williams, B. Hee Hong, J.-H. Ahn, J. Min Kim, H. Zirath, B. J. van Wees, H. van der Zant, L. Occhipinti, A. Di Matteo, I. A. Kinloch, T. Seyller, E. Quesnel, X. Feng, K. Teo, N. Rupesinghe, P. Hakonen, S. R. T. Neil, Q. Tannock, T. Lofwander, J. Kinaret, *Nanoscale* **2015**, 7, 4598-4810.
- [2] M. V. Fabretto, D. R. Evans, M. Mueller, K. Zuber, P. Hojati-Talemi, R. D. Short, G. G. Wallace, P. J. Murphy, *Chem. Mater.* **2012**, 24, 3998-4003.
- [3] M. Armand, S. Grugeon, H. Vezin, S. Laruelle, P. Ribière, P. Poizot, J. M. Tarascon, *Nat. Mater.* **2009**, 8, 120.
- [4] L. Fédèle, F. Sauvage, J. Bois, J.-M. Tarascon, M. Bécuwe, *J. Electrochem. Soc.* **2014**, 161, A46-A52.
- [5] X. Wu, J. Ma, Y.-S. Hu, H. Li, L. Chen, *J. Energ. Chem.* **2014**, 23, 269-273.
- [6] X. Han, G. Qing, J. Sun, T. Sun, *Angew. Chem. Int. Ed.* **2012**, 51, 5147-5151.
- [7] S. Wang, L. Wang, K. Zhang, Z. Zhu, Z. Tao, J. Chen, *Nano Lett.* **2013**, 13, 4404-4409.
- [8] R. R. Zhao, Y. L. Cao, X. P. Ai, H. X. Yang, *J. Electroanal. Chem.* **2013**, 688, 93-97.